

# Interaction between Flexible Buried Pipe and Surface Load

Yoo, Chung-Sik\*<sup>1</sup>      Chung, Suk-Won\*<sup>2</sup>

Lee, Kwang-Myung\*<sup>1</sup>    Kim, Joo-Suk\*<sup>2</sup>

---

## 요 지

본 논문에서는 연성 매설관과 지표 상재하중의 상호작용에 관한 내용을 다루었다. 본 연구에서는 유한요소해석을 이용한 매개변수 연구를 수행하였으며, 이와 아울러서 적용된 유한요소해석 모형의 검증 및 지표 상재하중을 부담하는 연성 매설관의 거동 파악을 목적으로 실내모형실험을 수행하였다. 해석결과를 토대로 지반/매설관 접촉면에서의 연직응력 및 파이프의 축력 분포 경향 등 지표 상재하중하에서 매설관의 하중응답 특성을 구체적으로 고찰하였으며, 그 결과를 종합적으로 분석하여 추후 수행될 보다 효율적인 매설관 설계/해석법의 개발에 사용될 데이터 베이스를 구축하였다. 해석결과를 분석한 결과 매설관과 지표 상재하중의 상호작용 정도는 매설관과 상재하중의 상대적 위치에 따라 좌우되며, 지반-구조물 상호작용을 고려하지 않고 있는 현 설계방법은 연성 매설관의 지표 상재하중에 대한 응답특성을 효율적으로 반영하지 못하는 것으로 나타났다. 또한 본 연구의 결과를 토대로 지표 상재하중에 의한 연성 매설관의 최대 축력을 예측할 수 있는 반경험적 평가식을 제시하였다.

## Abstract

This paper presents the results of a parametric study on the interaction between buried pipes and surface load using the finite element method of analysis. A series of laboratory model tests were also performed in order to validate the adopted finite element model and to capture essential features of the physical behavior of buried pipes subjected to surface load. In the parametric study, a wide range of boundary conditions were analyzed with emphasis on the response of the buried pipes to surface load. The results of analysis such as contact stress distribution at the soil/pipe interface and axial thrust of the pipe were thoroughly analyzed, and a database on the response of buried pipe under surface load was established for future development of a semi-empirical design/analysis method. The results indicated that the degree of interaction between buried pipes and surface load significantly varies with the vertical and lateral location of pipe with respect to surface load, and that the current design method, which does not consider soil-structure interaction, cannot correctly capture the pipe response to surface loading. Furthermore, based on the results of

---

\*1 Member, Associate Professor, Dept. of Civil Eng., Sungkyunkwan University

\*2 Graduate Student, Dept. of Civil Eng., Sungkyunkwan University

analysis, a semi-empirical equation was suggested, which estimates the maximum pipe thrust due to surface load for flexible buried pipes.

**Keywords:** Buried pipe, Finite element analysis, Surface load, Model test, Soil-structure interaction

---

## 1. Introduction

The rapid development of urban areas has resulted in an increased demand for construction of utilities for water or gas supplies, sewage disposals, and electric lines. Some of these utilities are constructed underground in the form of buried pipes, and are subjected to various types of surface load during its life time, such as traffic loads from vehicles or heavy equipment, and footing loads from newly constructed buildings. The interaction between a buried pipe and surface load may result in a structural damage to the pipe, and therefore a potential structural damage of buried pipe due to various forms of surface load must be evaluated during design and construction phases. To minimize such a potential structural damage requires a thorough understanding of the interaction mechanism between the buried pipe and surface load and a method for predicting the response of buried pipe to surface load. At present, however, the mechanism of pipe response to surface load is not fully understood.

Studies concerning the interaction between buried pipe and surface load are surprisingly limited. Fourie and Beer(1989) investigated the performance of a buried pipe with shallow cover under surcharge loading, and reported that the possibility of soil yield, merely treating the soil continuum as an elastic medium, will result in an interaction mechanism between soil and structure which may produce invalid estimates of pipeline stresses. Later, Chiou and Chi(1993) performed an extensive study on limit loads on buried pipelines in elastic soil medium using a variety of numerical modeling techniques. They concluded, among other things, that the limit load for a given buried pipe is influenced by several factors including surrounding ground condition, geometrical condition of pipe, and initial structural defects in pipe. More recently, Park et al.(1998) conducted a study on the deformation behavior of FC pipe buried in weathered soil under surface load using both physical and numerical modelings. In their study, various loading conditions were considered to capture the load response mechanism of buried pipe, and practical equations were developed for estimating the deformation of the FC pipe.

Although the aforementioned studies have given insight into the interaction mechanism between buried pipe and surface load, much still needs to be investigated for more thorough understanding of working mechanism of pipe response to surface load to be established. In view of this, this study was undertaken in response to such a research need. Particular emphases were placed on the surface load induced stress distributions around pipe and the response of pipe to surface loads. The implications of the findings from this study to current design approaches were also discussed in great detail.

## 2. Problems Considered

The geometry of the buried pipe system subjected to a surface strip load examined is shown in Figure 1 together with the various symbols used in this study. Due to the large number of variables and the complex interactions involved in this subject, it is essential to deal with a rather simple boundary condition before more complicated problems can be addressed. In view of this, a plane strain idealization was adopted by assuming that the pipe runs parallel to the axis of surface strip load. The results of analysis may, therefore, provide an upper bound for the pipe response.

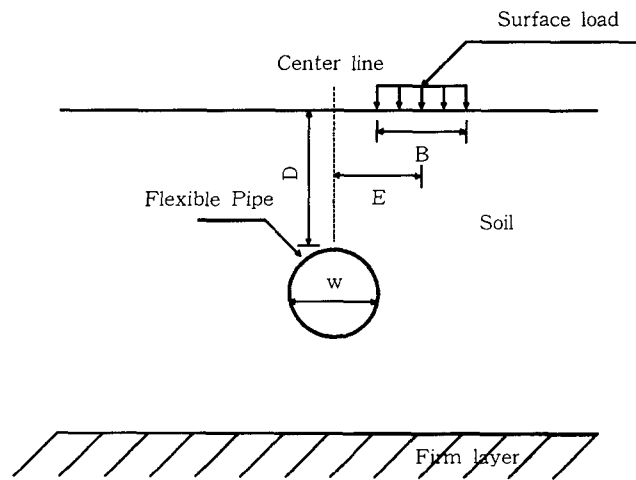


Figure 1. A schematic view of soil-pipe system

In the analysis, a 1.0m diameter rigid steel pipe with 5 mm thick walls installed in a trench was considered. It was assumed that after the installation of the pipe, the trench was backfilled with a weathered granite soil compacted to 95% of standard Proctor compaction, and that a uniformly distributed surface strip load was applied through a rigid plate over a finite width( $B$ ) of 1.0m. The material properties for the foundation soil and the buried pipe were taken from the available literatures and are summarized in Table 1.

Table 1. Material properties used in the finite element analysis

	Backfill	Buried pipe
Young's modulus, $E$ (kPa)	25,000	$2.0 \times 10^8$
Int. friction angle, $\psi$ (degree)	35	-
Cohesion, $c$ (kPa)	30	-
Unit weight, $\gamma$ (kN/m <sup>3</sup> )	20	-
Poisson's ratio, $\nu$	0.3	-
Area, $A$ (m <sup>2</sup> /m)	-	0.005

### 3. Finite Element Analysis

The preceding literature review indicates that the finite element analysis can successfully be used to analyze the pipe response to surface load. Therefore, the analysis of interaction between buried pipe and surface load was made using a plane strain finite element program GEOFE2D developed at Sungkyunkwan University. In the analysis, a wide range of boundary conditions by varying the burial depth ( $D/B = 1.0 \sim 6.0$ ) and pipe eccentricity ( $E/B = 0.0 \sim 4.0$ ) were considered in an attempt to capture the essential features of interaction mechanism between the pipe and the surface load.

In the finite element modeling, the entire soil-pipe system was represented as an assemblage of finite elements interconnected by a finite number of nodal points. The vertical and horizontal rollers were placed both at approximately  $6.0D$  and  $3.0D$ , respectively, from the pipe center to truncate the semi-infinite soil domain. For cases of which the pipe is off-centered with respect to the surface load, the vertical rollers were placed so that the distance between a lateral boundary and an edge of surface load might be maintained at least  $6.0D$ . Locations of these boundaries were selected in accordance with the results of preliminary analysis so that the presence of the artificial boundaries may not significantly alter the stress-strain field.

In the modeling, the original ground and backfill soil were treated as the same material and modeled using four-node isoparametric plane strain elements while two-node beam elements were used for the pipe. Figure 2 shows a typical finite element mesh used in the analysis, consisting of approximately 800 nodes and 600 elements. The soil was treated as an elasto-plastic material obeying the Mohr-Coulomb failure criterion together with the associated flow rule, whereas the pipe as a linear-elastic material. The assumption of the pipe's being linear elastic material was adequate since the intention was not to reproduce ultimate failure of the pipe, but rather to compare predictions at working load conditions.

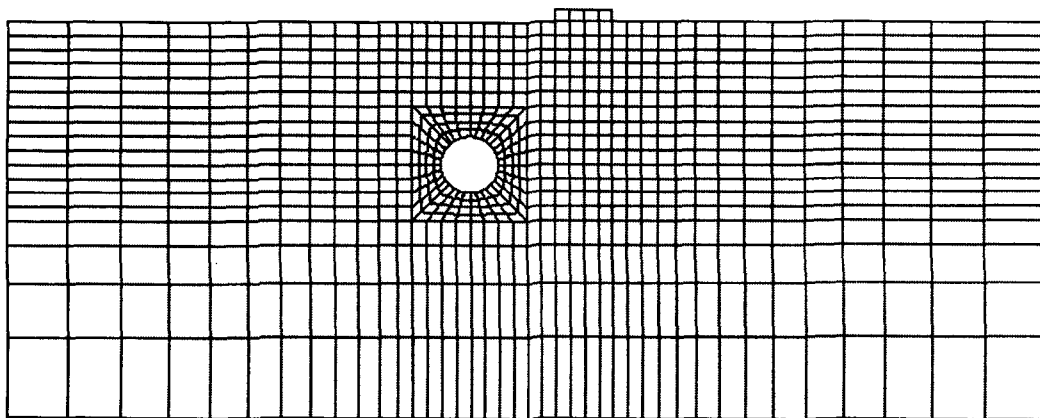


Figure 2. A typical finite element mesh used in the analysis

The initial stress condition before the surface loading was achieved by applying the gravity force caused by the soil weight with all the elements being active including the beam elements representing the pipe. This type of simplified single-step pipe installation approach is justified since this study was focused on the interaction between buried pipe and surface load, not on the behavior of pipe during installation. After achieving the initial condition, the surface load was then applied in increments through the loading plate.

#### 4. Validation of Finite Element Model

##### 4.1 Laboratory Model Tests

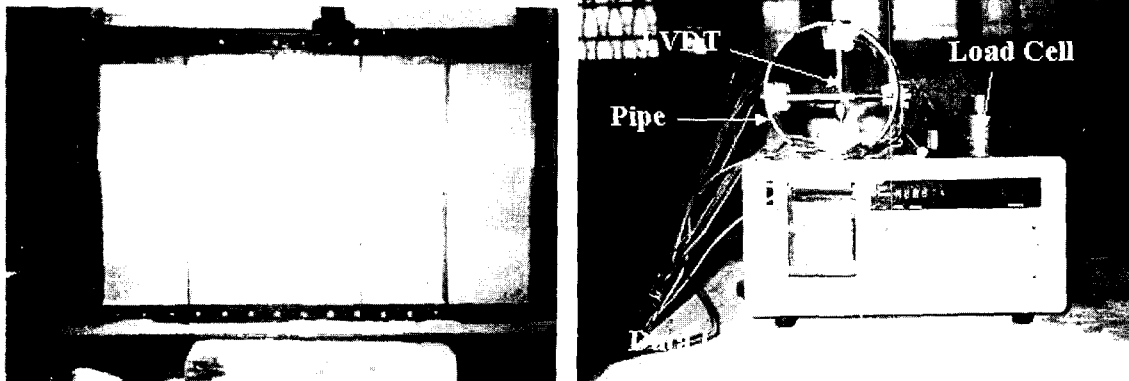
For the purpose of validating the finite element model adopted in this study and capturing the fundamental mechanism of pipe response to surface load, a series of laboratory model tests were conducted. The tests were conducted in a test box having an internal dimension of 1.8m(length) × 0.2m(width) × 1.2m(depth). The test box was encased with plexiglasses at four sides for ease of observing the soil movement inside the test box. Slip sheets were attached to the side walls of the test box to minimize possible friction between the ground and the wall. Four different conditions, two levels of pipe burial depth ( $D/B = 1.0, 3.0$ ) and pipe eccentricity ( $E/B = 0.0, 2.0$ ), were tested.

The artificial ground was created with standard sands using the raining technique so as to maintain the relative density of the rained ground at approximately  $D_r = 75 \sim 80\%$ . Note that the effective size ( $D_{10}$ ), uniformity coefficient ( $C_u$ ), and coefficient of uniformity ( $C_c$ ) for the sands were 0.36mm, 1.61, and 1.1, respectively. The consistency of the rained ground was assured by placing small cans at different locations during raining. A 135mm diameter circular plastic pipe with a thickness of 3mm was used to represent the buried pipe. The surface load was applied through a 20mm thick steel plate of 100mm(width) × 200mm(length) in size. The stress-strain and strength properties of the test soil were determined from the conventional triaxial compression test as well as direct shear test. The material properties for the test ground and the pipe are summarized in Table 2.

The test conditions were simulated using the finite element program GEOFE2D mentioned in the previous section. Note that the finite element model was constructed in accordance with the test configuration. The test procedure was carefully simulated in the finite element analysis as discussed in chapter 4.1. An extensive monitoring program was implemented to capture the essential features of the pipe response to surface load. Monitoring items include the surface load applied, the loading plate settlement, the pipe deflection and hoop strains, earth pressures around the pipe. Data acquisition was done using TDS-301 connected to a personal computer. Figure 3 shows photographs of the test box and the instrumentation setup.

Table 2. Material properties for the test ground and the pipe

	Test ground	Plastic pipe
Young's modulus, $E$ (kPa)	30.000	$2.7 \times 10^8$
Int. friction angle, $\psi$ (degree)	$38^\circ$	-
Cohesion, $c$ (kPa)	0	-
Unit weight, $\gamma$ (kN/m <sup>3</sup> )	16	-
Poisson's ratio, $\nu$	0.3	-
Area, $A$ (m <sup>2</sup> /m)	-	0.003



(a) Test box

(b) Instrumentation setup

Figure 3. Photographs of test box and instrumentation setup

#### 4.2 Comparison of Measured and Predicted Results

Measured pipe deflections and hoop strains were compared with the results of the finite element analysis. Note that the measurements for the pipe deflections were made at the pipe crown as well as springline levels while the hoop strains were measured at various locations around the pipe. Figure 4 compares the measured and computed relations between the surface load and the pipe deflection (i.e.  $q$  vs.  $\delta_{CR}$  and  $q$  vs.  $\delta_{SL}$ ) for  $E/B=0.0$  and  $E/B=2.0$  with  $D/B=1.0$ . As can be seen in this figure, fairly close agreement between the measured and computed results for both pipe crown and springline convergence can be observed with some discrepancies at ultimate level. The discrepancies may be attributed to the nonlinear material behavior of the pipe under the loading. Inspection of the measured and computed curves reveals that the case with  $E/B$  demonstrates a markedly stiffer response (i.e. less pipe deflection under a given surface load). This trend, as one can expect, is due to less interaction between the pipe and surface load.

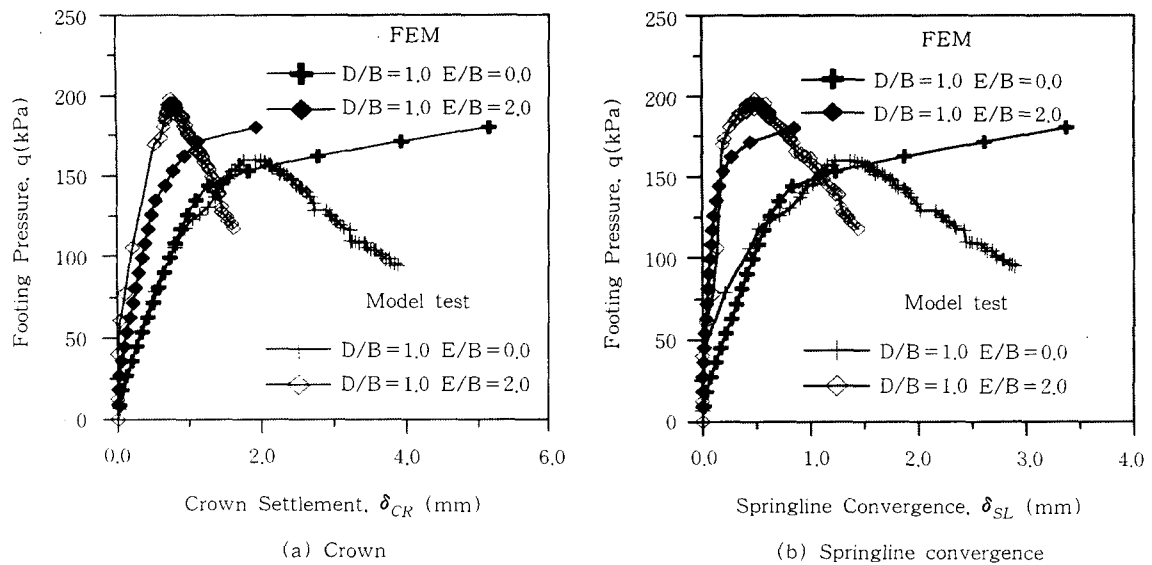


Figure 4. Measured and predicted  $q$  vs.  $\delta_{pipe}$  relations ( $D/B = 1.0$ )

Figure 5 illustrates the measured and predicted pipe hoop strains under a surface pressure of 150 kPa. As seen in this figure, although there exists considerable discrepancies between the measured and predicted strains, the trend of decreasing strain levels with increasing  $E/B$  can be observed in the two sets of data. In addition, the predicted distribution patterns agree well with the measured results, showing the maximum strains occurring at  $\pm 60^\circ$  from the vertical and at the crown level for  $E/B = 0.0$  and  $E/B = 2.0$ , respectively. Although the reasons for such discrepancies are not immediately clear, the calibration error for the strain gauges and the possible slip at the soil/pipe interface may be responsible.

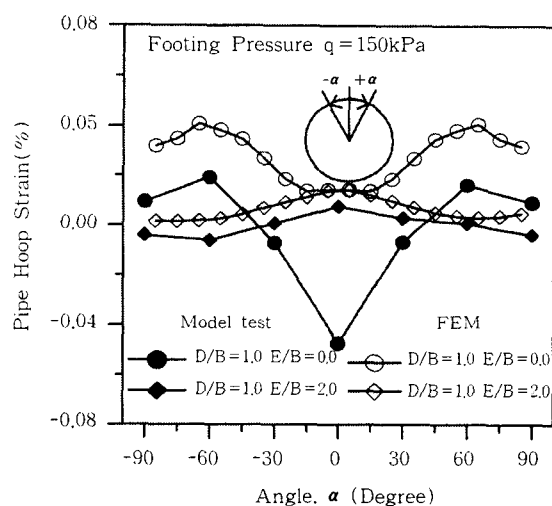


Figure 5. Measured and predicted pipe hoop strains at  $q = 150$  kPa ( $D/B = 1.0$ )

As demonstrated, the predicted results match fairly well with the measured ones, although some discrepancies are observed. Such discrepancies may not appear to be severe considering the range of uncertainties in a soil-structure interaction problem such as that described in this study. Thus the finite element model described in section 3 was adopted to analyze the pipe-surface load interaction problem described earlier.

## 5. Results and Discussions

The results of the parametric study for the problem described in section 3 were analyzed in an attempt to investigate the pipe response to the surface load. What is examined include normal contact stresses at soil-pipe interface and pipe thrust. Note that the surface load induced results obtained under the surface load of 600kPa were used for discussion. The surface load of 600 kPa corresponds to the allowable bearing capacity with a factor of safety 2.0 for the foundation soil, and therefore, the presented results in subsequent paragraphs may be regarded as relevant to working load conditions.

### 5.1 Normal Contact Stresses at Soil-Pipe Interface

The normal contact stresses at the soil-pipe interface are greatly influenced by the deflected shape of the pipe. Figure 6 illustrates the deflected shapes for the centered ( $E/B=0.0$ ) and the off-centered ( $E/B=2.0$ ) cases for  $D/B=1.0$ . The distinctive features for  $E/B=0.0$  are a flattening of the crown as well as an outwards bulge at the springline of the pipe, as expected. The deflected shape for  $E/B=2.0$ , however, exhibits different pattern, showing the maximum deflection at the pipe shoulder, i.e.  $+45^\circ$  from the vertical, caused primarily by asymmetrical loading.

Corresponding normal contact stress distributions are shown in Figure 7. As expected, for  $E/B=0.0$ , the maximum normal contact stress occurs at  $\pm 30^\circ$  from the vertical. Thereafter, there is

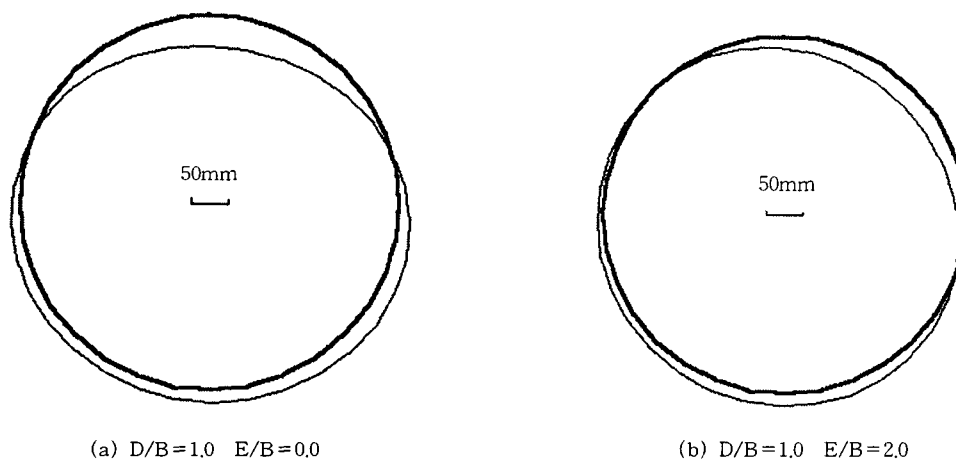


Figure 6. Deflected shapes of the pipe ( $D/B=1.0$ )



a rapid decrease with a minimum value at about 45° from the vertical. Between 45° and 90° to the vertical, the contact stress builds up rapidly to a maximum of 500kPa, caused by the outward bulging of the pipe. The pattern of the normal contact stress distribution corresponds well to the deformed shape of the pipe and the maximum shear strain ( $\epsilon_1 - \epsilon_3$ ) contour shown in Figure 8, illustrating that the possible failure surface extends to the locations where the maximum normal contact stresses occur. The distribution pattern for  $E/B=2.0$ , however, exhibits not only much lower normal contact stresses but also significantly different pattern showing the local maximum at the right shoulder and invert. This trend again agrees fairly well with the deflected shape as presented, in Figure 6.

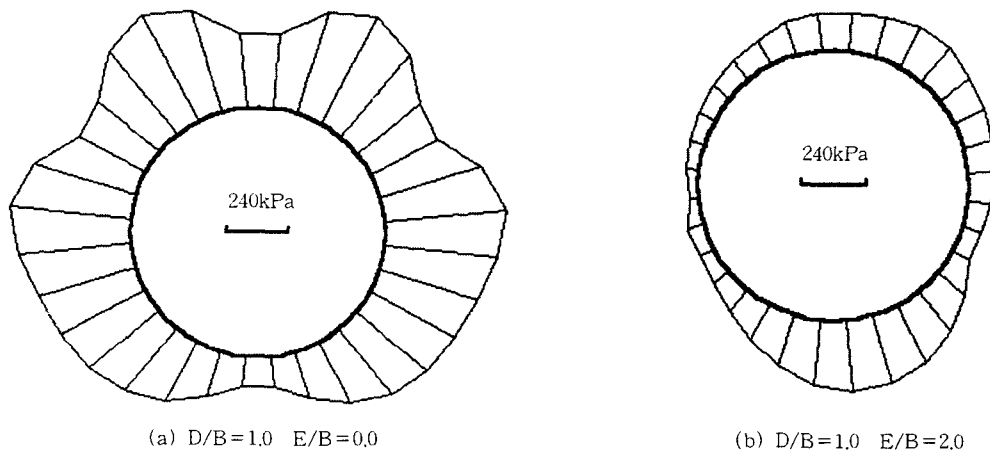


Figure 7. Normal contact stress distributions around the pipe ( $D/B=1.0$ )

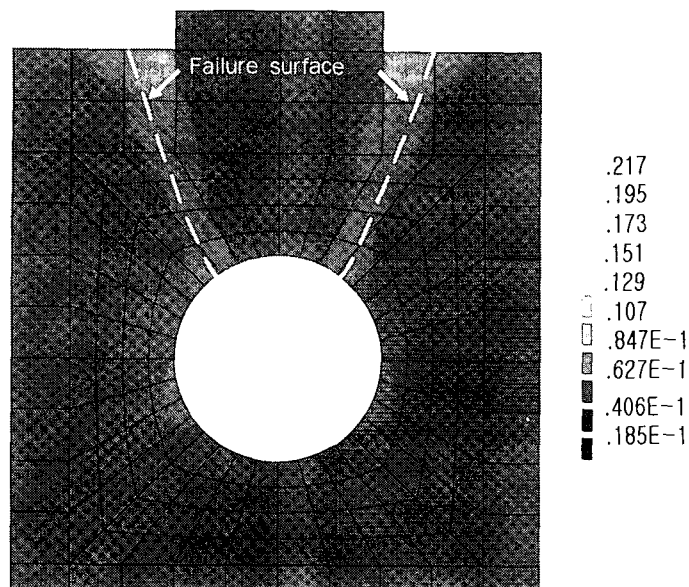


Figure 8. Maximum shear strain ( $\epsilon_1 - \epsilon_3$ ) contour for  $D/B=1.0$  and  $E/B=0.0$

## 5.2 Pipe Response to Surface Load

Structural behavior of the pipe may be assessed by means of circumferential thrusts and bending moments. Due to low flexural rigidity of the pipe, only the circumferential thrusts were examined in this study. Figures 9 and 10 illustrate the variations of the pipe thrusts with  $D/B$  and  $E/B$ , respectively. Note that the normalized pipe thrusts by the surface load ( $N/qB$ ) are used for discussion. It can be seen in Figure 9, which shows the variation with  $D/B$  for the centrally loaded case ( $E/B=0.0$ ), that the maximum thrusts occur at  $\pm 60^\circ$  from the vertical, and that the level of  $N/qB$  significantly decreases with increasing  $D/B$  at a decreasing rate. This trend, to a large extent, is a direct consequence of diminishing effect of the surface load on the pipe with increasing  $D/B$ , as one can expect. Furthermore, it is of interest to note that no significant variation with  $D/B$  is observed when  $D/B > 4.0$ . This trend in turn indicates that no interaction between the pipe and the surface load can be assumed when  $D/B > 4.0$ .

For cases with  $E/B$ , the distribution patterns are considerably different from those with  $E/B=0.0$ , showing the local maximum at  $+120^\circ$  and  $-30^\circ$  from the vertical, as illustrated in Figure 10. The general variation with  $E/B$ , however, is similar to that with  $D/B$ , showing the decreasing level of  $N/qB$  with increasing  $E/B$ . It appears that the surface load ceases its influence when  $E/B > 4.0$ , showing negligibly small value of  $N/qB$ .

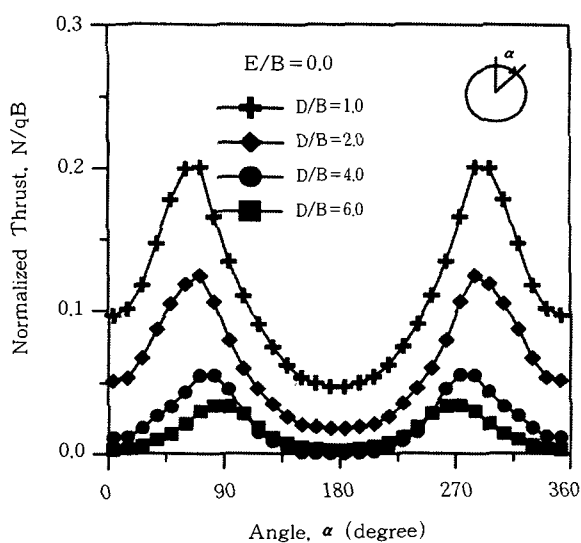


Figure 9. Variation of normalized pipe thrusts ( $N/qB$ ) distribution with  $D/B$

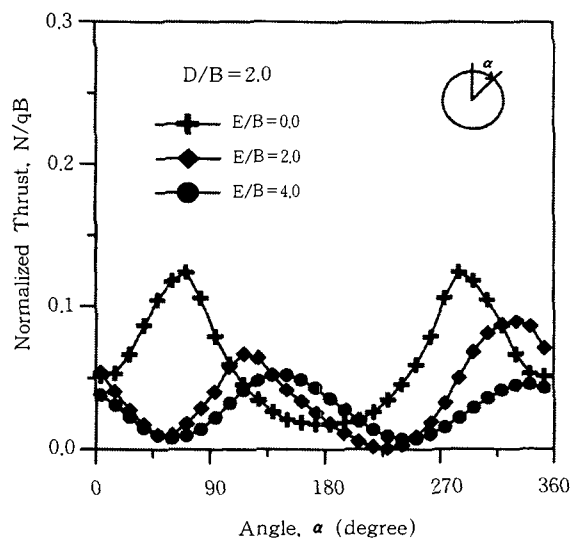


Figure 10. Variation of normalized pipe thrusts ( $N/qB$ ) distribution with  $E/B$

The variation of pipe response to surface load with the ground conditions was investigated by varying the elastic modulus ( $E_s$ ) of the foundation soil from 15,000 to 60,000 kPa. Figure 11 shows the variation of  $N/qB$  distribution with  $E_s$  for  $E/B=0.0$ . As illustrated in this figure, the elastic modulus of the soil does not appear to influence the pipe performance, showing almost constant

pipe thrusts regardless of  $E_s$ . Although more detailed analysis is required to draw a conclusion, this trend may be attributed to the flexibility of the pipe and implies that the soil elastic modulus can be discounted when estimating the pipe thrust.

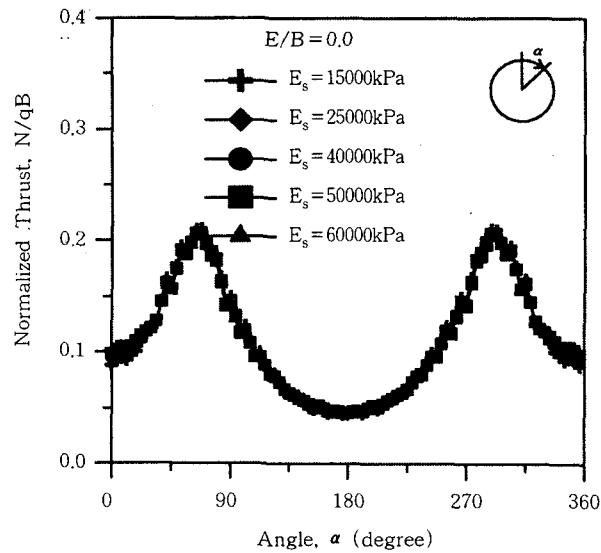


Figure 11. Variation of normalized pipe thrusts ( $N/qB$ ) distribution with soil modulus  $E_s$

The relationships between the maximum pipe thrust ( $N_{max}$ ) and the applied surface load ( $qB$ ) are illustrated in Figures 12 and 13 for various  $D/B$  and  $E/B$ . Also included are the computed results from the equation (1), which is based on the ring theory.

$$N_{max} = \frac{P_v D}{2} \quad (1)$$

where  $P_v$  and  $D$  are the vertical pressures at the crown level caused by surface load and the pipe diameter, respectively. Note that Boussinesq solution is usually adopted in calculating the  $P_v$ . As expected, it is seen that the  $N_{max}$  vs.  $qB$  relations follow linear trend, and that the slope of  $N_{max}$  vs.  $qB$  curve decreases as  $D/B$  or  $E/B$  increases, which implies less influence on the pipe performance. Again, in Figure 12, no significant differences are observed between  $D/B=4.0$  and  $6.0$ , indicating negligible influence of the surface load. Furthermore, the equation (1) tends to underestimate the pipe thrust, showing much smaller  $N_{max}$  than that from the finite element analysis, except for  $D/B=1.0$ . Similar trend can be observed in Figure 13, which illustrates the variation of  $N_{max}$  vs.  $qB$  relation with  $E/B$  for  $D/B=2.0$ . As expected, the relations follow linear trend and the slope of the curve decreases with increasing  $E/B$ . Again, the equation (1) yields much smaller  $N_{max}$  when compared to those from the finite element analysis.

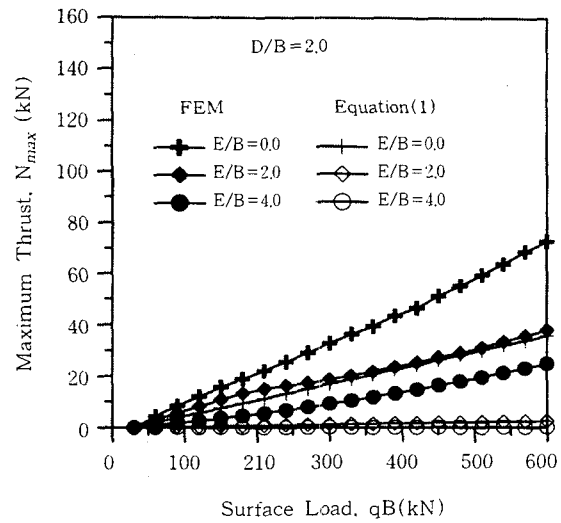
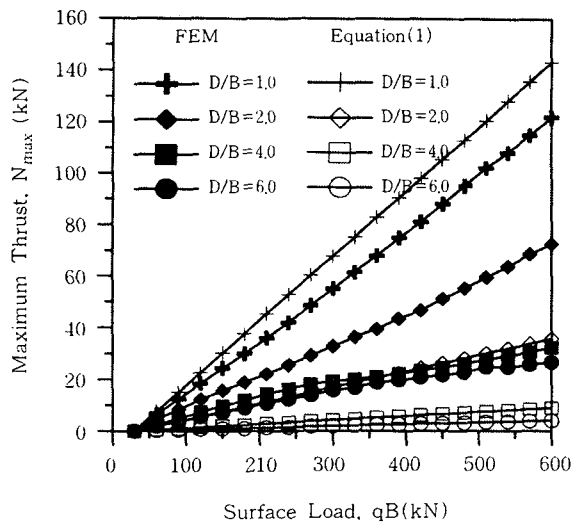


Figure 12. Variation of  $N_{max}$  vs.  $qB$  relations with  $D/B$  Figure 13. Variation of  $N_{max}$  vs.  $qB$  relations with  $E/B$

The response of the pipe to the surface load is further analyzed using the variation of the normalized maximum pipe thrust ( $N_{max}/qB$ ) with  $D/B$  for various  $E/B$  in Figure 14. As seen in this figure, a general trend of decreasing  $N_{max}/qB$  with increasing  $D/B$  is evident for  $E/B=0.0$ . As has been observed,  $N_{max}/qB$  becomes constant beyond  $D/B=4.0$ , indicating little or no influence of the surface load on the pipe. Furthermore, the curves for the cases with  $E/B$  exhibit almost constant value, suggesting negligibly small influence of the surface load. Comparison between the results from the equation (1) and the predicted ones reveals that the equation (1), in general, tends to significantly underestimate the pipe thrust  $N_{max}/qB$  with this trend being more pronounced as  $D/B$  and  $E/B$  increase. A possible reason for such trend may be that the soil-structure interaction is not taken into consideration in the current design approach.

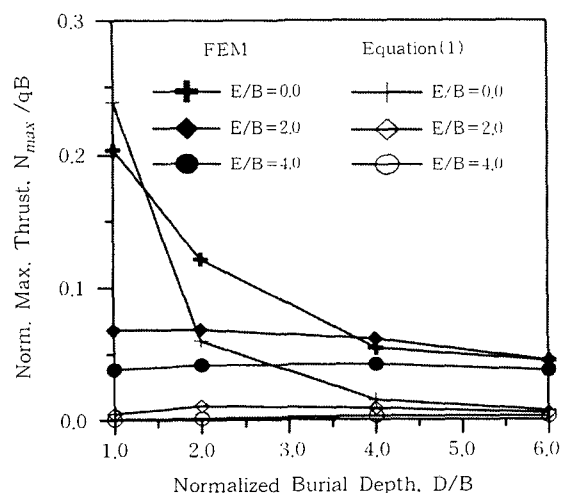


Figure 14. Variation of normalized maximum pipe thrust ( $N_{max}/qB$ ) with  $D/B$

Based on the results presented above, an attempt was made to develop an equation for estimating  $N_{max}/qB$  for a given pipe condition. Since the possible maximum pipe thrust for a given loading condition is of great concern for design, only the results for the cases with  $E/B=0.0$  were considered. In addition, since the results of analysis indicated the linear relation between the pipe thrust and the level of applied surface load, the burial depth  $D/B$  was taken as the single variable. The equation (2) was then developed using the multiple regression analysis on the data base for  $N_{max}/qB$  versus  $D/B$ . Note that the coefficient of determination  $R^2$  was approximately 98%, indicating very high correlation between  $N_{max}/qB$  and  $D/B$ . Figure 15 compares the computed by equation (2) with the predicted results. As can be seen, the two sets of data show very good agreement, and therefore, the pipe thrust  $N_{max}/qB$  can be estimated using the equation (2) for the conditions similar to that considered in this study.

$$\frac{N_{max}}{qB} = 0.21 \left( \frac{D}{B} \right)^{-0.89} \quad (2)$$

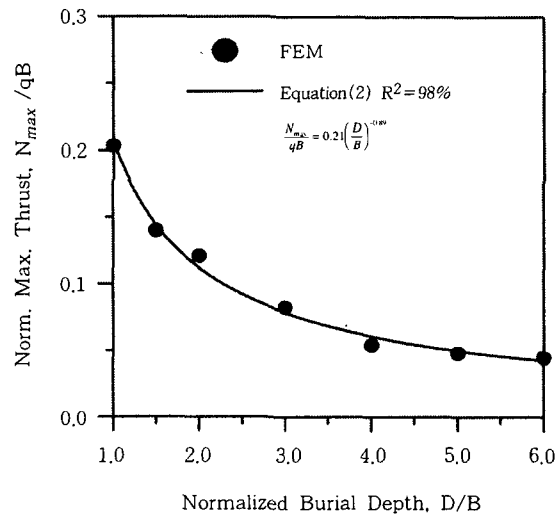


Figure 15. Comparison between Equation (2) and predicted results

### 5.3. Practical Implications

The results of the parametric study have revealed insights into structural response of the flexible buried pipe to surface load. Practical implications of the findings from this study are discussed hereunder.

As revealed, the current design approach based on the Boussinesq solution, in general, tends to underestimate the pipe thrust caused by surface loading. This trend becomes more pronounced as  $D/B$  and  $E/B$  increase. This results in turn suggest that a care should be taken when using the current design approach for the cases with high level of surface load, since the degree to which the

current design approach underestimates the pipe response would increase with the increase of the level of surface load.

Furthermore, the results of analysis indicated that the influence of the surface load may be ignored when  $D/B > 4.0$  or  $E/B > 2.0$ . These limits of no influence appear to be greater than those based on the conventional design approach, which suggests ignoring the vehicle load when the burial depth exceeds 2.4m. This may be because the conventional design approach does not take the soil-structure interaction into consideration.

## 6. Conclusions

The interaction between buried pipes and surface loads was investigated using the finite element method of analysis with the aim of establishing a database for future development of a more rational design method for buried pipes under various conditions. A series of reduced small scale model tests were also performed in order to validate the adopted finite element model. Based on the findings from this study, the following conclusions may be drawn.

1. The pipe response to the surface load significantly varies with the burial depth of the pipe  $D/B$  as well as the lateral distance from the surface load to the pipe  $E/B$ . Furthermore, the influence of surface load may be ignored when  $D/B \geq 4.0$  or  $E/B \geq 2.0$ . When the pipe is located outside the limits, the effect of soil-pipe interaction should be considered in the pipe design.

2. The current design method based on the Boussinesq solution tends to underestimate the pipe thrust caused by the surface load with this trend being more pronounced as  $D/B$  or  $E/B$  increases. The fact that the current design method does not take the soil-pipe interaction into consideration may be responsible for such trend.

3. Based on the results obtained from the study, a semi-empirical equation for estimating the pipe thrust has been developed. Maximum pipe thrust caused by a surface load can therefore be determined using the developed equation at least within the range of conditions investigated.

## Acknowledgement

Financial support for this research provided by SAFE(SAFETY and Structural Integrity Research Center) at Sungkyunkwan University is gratefully acknowledged.

## References

1. Park, J. B., Chung, C. K., Kwon, H. J., Choe, M. J., and Kim, J. S.(1998). "Deformation behavior of pipe buried in weathered soil under surface load", J. of Civil Engrg., KSCE, Vol 18, No. III-3, pp. 391-402.
2. Chiou, Y. J. and Chi, S. Y.(1993), "Limit loads of buried pipelines in inelastic soil medium", J. of Engrg. Mech., ASCE, Vol. 119, No. 5, pp. 938-954.
3. Davis, R. E.(1986). "Rigid culvert finite element analysis," J. of Geotech. Engrg., ASCE, Vol. 112(8), pp.

749-767.

4. Fourie, R. A. and Beer, G.(1989). "An illustration of the importance of soil non-linearity in soil-structure interaction problems." *Computers and Geotechnics*, Vol. 8, pp. 219-241.
5. Jiang, N. (1987). "New design procedure for underground vitrified clay pipes." Ph.D. Thesis, The University of Wisconsin-Madison.
6. Roschke, P. N. and Davis, R. E.(1987). "Rigid culvert finite element analyses", *J. Geotech. Engrg., ASCE*, Vol. 112, No. 8, pp. 749-767.
7. Selig, E. T., McVay, M. C., and Chang, C. S.(1982). "Finite element modeling of buried concrete pipe installations." *Soil-Structure Interaction of Subsurface Conduits, Transp. Res. Rec.* 878, pp. 17-23.
8. Selig, E. T., and Packard, D. L.(1986). "Buried concrete pipe embankment installation analysis." *J. Transp. Engrg., ASCE*, Vol. 112, No. 6, pp. 576-592.
9. Selig, E. T., and Packard, D. L.(1988). "Buried concrete pipe trench installation analysis." *J. Geotech. Engrg., ASCE*, Vol. 113, No. 5, pp. 485-501.

(received on Apr., 10. 1999)